Proximity effect in superconductor / conical magnet heterostructures

Daniel Fritsch and James F. Annett

H. H. Wills Physics Laboratory, School of Physics, University of Bristol, Bristol BS8 1TL, UK

E-mail: daniel.fritsch@bristol.ac.uk

Abstract. The presence of a spin-flip potential at the interface between a superconductor and a ferromagnetic metal allows for the generation of equal-spin spin-triplet Cooper pairs. These Cooper pairs are compatible with the exchange interaction within the ferromagnetic region and hence allow for the long-range proximity effect through a ferromagnet or half-metal. One suitable spin-flip potential is provided by incorporating the conical magnet Holmium (Ho) into the interface. The conical magnetic structure is characterised by an opening angle α with respect to the crystal c-axis and a turning (or pitch) angle β measuring the rotation of magnetisation with respect to the adjacent layers. Here, we present results showing the influence of conical magnet interface layers with varying α and β on the efficiency of the generation of equal-spin spin-triplet pairing. The results are obtained by self-consistent solutions of the microscopic Bogoliubov—de Gennes equations in the clean limit within a tight-binding model of the heterostructure. In particular, the dependence of unequal-spin and equal-spin spin-triplet pairing correlations on the conical magnetic angles α and β are discussed in detail.

PACS numbers: 74.45.+c,74.78.Fk,74.20.-z,74.20.Mn

Submitted to: J. Phys.: Condens. Matter

1. Introduction

The interface of a superconductor (SC) and a ferromagnetic metal (FM) is a source of many intriguing phenomena [1, 2, 3, 4]. Unlike the case of the proximity effect between a SC and a normal metal, there is oscillation of the decaying Cooper pair density in the ferromagnetic region of the heterostructure. This oscillation occurs because of the slightly different Fermi wave-vectors of the electrons of different spin in the FM. In the SC/FM proximity effect these oscillations occur for both the spin-singlet part of the pairing correlation, and also for the opposite spin (m = 0 relative to the FM magnetisation direction) part of the spin-triplet pairing correlations. Both of these parts of the pairing correlations are strongly suppressed by non-magnetic disorder in the FM and so lead to only a short ranged proximity effect in SC/FM heterostructures. If, however, the SC/FM interface allows for some kind of spin-flip process, then in addition to these singlet and opposite-spin triplet Cooper pair correlations it is also possible that equal-spin spin-triplet pairing correlations ($m = \pm 1$) can be generated at the interface. Such pairing correlations are compatible with the ferromagnetic

exchange interaction [5] and hence do not oscillate or decay in the FM region. These equal-spin spin-triplet pairing correlations thus allow for the long-range proximity effect, which is observed in certain SC/FM heterostructures. A review summarising the proximity effect in SC/FM heterostructures is provided by Buzdin [1], whereas Bergeret et al. [2] and Tanaka et al. [3] discuss in detail this new type of "odd-triplet" superconductivity and Eschrig et al. [4] provide detailed information about the underlying symmetry relations.

Experimentally, several different approaches to provide a spin-flip process at the interface have been proposed and proven to generate long-ranged SC/FM proximity effects. Here we specifically focus on the case where the necessary spin-flip scattering potential is provided by conical magnetic interface layers. Long-ranged proximity effects have been observed in experiments on heterostructures containing the conical ferromagnet Holmium (Ho), by Sosnin et al. [6], Halász et al. [7, 8], and Robinson et al. [9]. Theoretically, Ho containing heterostructures have been investigated by Alidoust et al. [10], Wu et al. [11] and in our previous work [12]. These calculations confirm that the conical magnet acts as a suitable spin-flip potential and generates equal-spin spin-triplet pairing correlations which extend far into the FM region, providing the microscopic basis for the long ranged proximity effect in such heterostructures.

The aim of this paper is to investigate in greater detail a single interface between an SC and a conical magnet (CM). The conical magnetic structure of Ho is characterised by the opening angle $\alpha = 80^{\circ}$ measuring the deviation of magnetisation from the c-axis growth direction (assumed normal to the SC/FM interface) and a turning (or pitch) angle $\beta = 30^{\circ}$ describing the magnetisation rotation between adjacent Ho layers. All previous theoretical investigations of SC/CM proximity effects focus on heterostructures containing Ho, and so naturally the conical magnetic angles α and β have been kept fixed to their respective Ho values. Consequently, an overall picture of the effectiveness of equal-spin spin-triplet generation of Ho compared to other possible conical magnetic interface materials has not emerged yet. Here we present calculations showing the influence of conical magnetic interface layers with varying α and β on the efficiency of equal-spin spin-triplet generation. We examine SC/CM interfaces in which the conical magnet parameters α and β are varied in the ranges of 0° to 180° . We have performed calculations for the full range of α and β angles with a step size of 5°. For each of the parameter sets the microscopic Bogoliubov—de Gennes (BdG) equations have been solved self-consistently in the clean limit.

The paper is organised as follow. Section 2 provides the theoretical background, including the necessary description of the microscopic BdG equations in section 2.1, and the method used to calculate the spin-triplet pairing correlations in section 2.2. Starting with the conical magnetic structure of Ho ($\alpha=80\,^{\circ}$ and $\beta=30\,^{\circ}$) we first show, in section 3.1, results for these values of α and β to introduce the key calculated quantities and our basic notations. Keeping α fixed the influence of varying β is then discussed in section 3.2. Finally section 3.3 shows results obtained for varying both α and β simultaneously. A summary and outlook are provided in the conclusion section 4.

2. Theoretical Background

2.1. Bogoliubov-de Gennes equations and heterostructure setup

The results presented below utilise self-consistent solutions of the microscopic BdG equations in the clean limit. The method employed is similar to our previous work on Ho containing heterostructures [12], so only the most relevant formulas are repeated here. Generally, the spin-dependent BdG equations can be written as [12, 13, 14, 15]

$$\begin{pmatrix}
\mathcal{H}_{0} - h_{z} & -h_{x} + ih_{y} & \Delta_{\uparrow\uparrow} & \Delta_{\uparrow\downarrow} \\
-h_{x} - ih_{y} & \mathcal{H}_{0} + h_{z} & \Delta_{\downarrow\uparrow} & \Delta_{\downarrow\downarrow} \\
\Delta_{\uparrow\uparrow}^{*} & \Delta_{\downarrow\uparrow}^{*} & -\mathcal{H}_{0} + h_{z} & h_{x} + ih_{y} \\
\Delta_{\uparrow\downarrow}^{*} & \Delta_{\downarrow\downarrow}^{*} & h_{x} - ih_{y} & -\mathcal{H}_{0} - h_{z}
\end{pmatrix}
\begin{pmatrix}
u_{n\uparrow} \\
u_{n\downarrow} \\
v_{n\uparrow} \\
v_{n\downarrow}
\end{pmatrix} = \varepsilon_{n} \begin{pmatrix}
u_{n\uparrow} \\
u_{n\downarrow} \\
v_{n\uparrow} \\
v_{n\downarrow}
\end{pmatrix} . (1)$$

Here, ε_n denotes the eigenvalues, and $u_{n\sigma}$ and $v_{n\sigma}$ are quasiparticle and quasihole amplitudes for spin σ , respectively. After some simplifications [12, 13, 16] the tight-binding Hamiltonian \mathcal{H}_0 reads

$$\mathcal{H}_0 = -t \sum_n \left(c_n^{\dagger} c_{n+1} + c_{n+1}^{\dagger} c_n \right) + \sum_n \left(\varepsilon_n - \mu \right) c_n^{\dagger} c_n , \qquad (2)$$

with c_n^{\dagger} and c_n being electronic creation and destruction operators at multilayer index n, respectively. Choosing the next-nearest neighbour hopping parameter t=1 and the chemical potential (Fermi energy) $\mu=0$ sets the energy scales.

The vector components of the conical exchange field are written as [10, 11, 12]

$$\mathbf{h} = h_0 \left\{ \cos \alpha \mathbf{y} + \sin \alpha \left[\sin \left(\frac{\beta y}{a} \right) \mathbf{x} + \cos \left(\frac{\beta y}{a} \right) \mathbf{z} \right] \right\}, \tag{3}$$

with $h_0 = 0.1$ being the strength of the conical magnet's exchange field and a = 1 being the lattice constant.

The general form of the pairing matrix in (1) can be rewritten according to Balian and Werthamer [17, 18]

$$\begin{pmatrix} \Delta_{\uparrow\uparrow} & \Delta_{\uparrow\downarrow} \\ \Delta_{\downarrow\uparrow} & \Delta_{\downarrow\downarrow} \end{pmatrix} = (\Delta + \hat{\sigma} \cdot \mathbf{d}) \, i \hat{\sigma}_2 = \begin{pmatrix} -d_x + i d_y & \Delta + d_z \\ -\Delta + d_z & d_x + i d_y \end{pmatrix}, \quad (4)$$

with $\hat{\cdot}$ indicating a 2×2 matrix. Utilising the Pauli matrices $\hat{\sigma}$, the superconducting order parameter is described by a singlet (scalar) part Δ and a triplet (vector) part \mathbf{d} , respectively.

In our model the pairing interaction is assumed to apply only for s-wave singlet Cooper pairs, and so the pairing potential is restricted to a scalar quantity Δ . This fulfils the self-consistency condition

$$\Delta(\mathbf{r}) = \frac{g(\mathbf{r})}{2} \sum_{n} \left(u_{n\uparrow}(\mathbf{r}) v_{n\downarrow}^*(\mathbf{r}) [1 - f(\varepsilon_n)] + u_{n\downarrow}(\mathbf{r}) v_{n\uparrow}^*(\mathbf{r}) f(\varepsilon_n) \right), \quad (5)$$

where we are summing only over positive eigenvalues ε_n , and where $f(\varepsilon_n)$ denotes the Fermi distribution function evaluated as a step function for zero temperature. Setting up the heterostructure as shown in figure 1 the effective superconducting coupling parameter $g(\mathbf{r})$ equals 1 in the $n_{\rm SC}=250$ layers of spin-singlet s-wave superconductor to the left of the interface and vanishes elsewhere. The conical exchange field, defined according to (3), is added to the $n_{\rm CM}=500$ layers of conical magnet to the right of the interface.

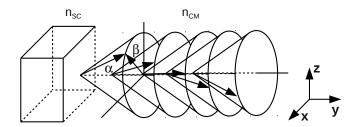


Figure 1. Setup of heterostructure consisting of a spin-singlet s-wave superconductor ($n_{\rm SC}=250$ layers), and a conical magnet ($n_{\rm CM}=500$ layers). The opening and turning angles α and β of the conical magnet are defined as shown. From (3) it follows that α is measured from +y towards +z, whereas β is measured from +z towards +x in the coordinate system indicated.

2.2. (Triplet) Pairing correlations

The superconducting pairing correlation between spins α and β can generally be evaluated as on-site interaction for times $t = \tau$ and t' = 0 as

$$f_{\alpha\beta}(\mathbf{r},\tau,0) = \frac{1}{2} \langle \hat{\Psi}_{\alpha}(\mathbf{r},\tau) \hat{\Psi}_{\beta}(\mathbf{r},0) \rangle, \qquad (6)$$

with $\hat{\Psi}_{\sigma}(\mathbf{r},\tau)$ being the many-body field operator for spin σ at time τ . The time-dependence is introduced through the Heisenberg equation of motion. Being local in space the pairing correlation evaluated using (6) leads to vanishing triplet contribution for $\tau = 0$ in accordance with the Pauli principle [19]. However for finite times τ nonvanishing contributions emerge, an example of odd-frequency triplet pairing [2]. Substituting the field operators valid for our setup and phase convention the spin-dependent triplet pairing correlations are given by

$$f_{0}(y,\tau) = \frac{1}{2} \left(f_{\uparrow\downarrow}(y,\tau) + f_{\downarrow\uparrow}(y,\tau) \right) = \frac{1}{2} \sum_{n} \left(u_{n\uparrow}(y) v_{n\downarrow}^{*}(y) + u_{n\downarrow}(y) v_{n\uparrow}^{*}(y) \right) \zeta_{n}(\tau)$$

$$f_{1}(y,\tau) = \frac{1}{2} \left(f_{\uparrow\uparrow}(y,\tau) - f_{\downarrow\downarrow}(y,\tau) \right) = \frac{1}{2} \sum_{n} \left(u_{n\uparrow}(y) v_{n\uparrow}^{*}(y) - u_{n\downarrow}(y) v_{n\downarrow}^{*}(y) \right) \zeta_{n}(\tau)$$

$$(7)$$

depending on position y and time parameter τ (set to $\tau = 10$ in the present numerical work), and with $\zeta_n(\tau)$ given by

$$\zeta_n(\tau) = \cos(\varepsilon_n \tau) - i \sin(\varepsilon_n \tau) (1 - 2f(\varepsilon_n)). \tag{8}$$

The pairing amplitudes in (7) are defined relative to a single spin-quantisation direction, here z. In the SC/FM proximity effect this has a natural choice as the FM spin direction. However in the present calculations for a SC/CM interface there is no such fixed reference axis, since the rotation of the CM moment leads to a spatially varying local magnetisation direction. Therefore it is helpful to represent the triplet pairing correlations in a form which is independent of the spin-quantisation axis chosen. Recalling (4) we define $\hat{\Delta}$ as the triplet pairing matrix for an ordinary spin-triplet superconductor

$$\hat{\Delta} = (\hat{\sigma} \cdot \mathbf{d}) \, i\hat{\sigma}_2 = \begin{pmatrix} -d_x + id_y & d_z \\ d_z & d_x + id_y \end{pmatrix} \,, \tag{9}$$

which obeys the following identity [18]

$$\hat{\Delta}\hat{\Delta}^{\dagger} = |\mathbf{d}|^2 \hat{\sigma}_0 + i \left(\mathbf{d} \times \mathbf{d}^*\right) \cdot \hat{\sigma}, \tag{10}$$

where $\hat{\sigma}_0$ denotes the identity matrix. For bulk triplet superconductors unitary pairing states are defined by the condition $i\mathbf{d} \times \mathbf{d}^* = 0$ and for these states $2|\mathbf{d}|$ is the quasiparticle energy gap. For non-unitary triplet states $i\mathbf{d} \times \mathbf{d}^* \neq 0$ and is a (real) vector in the direction of the net Cooper pair spin, i.e., it is a measure of the pair spin magnetic moment [18, 10]. The quantities $|\mathbf{d}|$ and $i\mathbf{d} \times \mathbf{d}^*$ are obviously also gauge invariant, unlike the complex vector \mathbf{d} itself.

In the present work there is no pairing interaction in the triplet channel, (5), and so $\mathbf{d} = 0$. Therefore, instead of this we focus on the triplet pair correlation function matrix which can be written similarly to the matrix (9) as [20, 10]

$$\hat{f} = (\hat{\sigma} \cdot \mathbf{f}) \, i\hat{\sigma}_2 = \begin{pmatrix} -f_x + if_y & f_z \\ f_z & f_x + if_y \end{pmatrix} . \tag{11}$$

(Note the additional factor i in this definition compared to [20] to be consistent with the definition of $\hat{\Delta}$ in (4).) Now the analogue to (10) reads

$$\hat{f}\hat{f}^{\dagger} = |\mathbf{f}|^2 \hat{\sigma}_0 + i \left(\mathbf{f} \times \mathbf{f}^*\right) \cdot \hat{\sigma}. \tag{12}$$

The two analogues to $|\mathbf{d}|$ and $\mathbf{d} \times \mathbf{d}^*$, namely $|\mathbf{f}|$ and $\mathbf{f} \times \mathbf{f}^*$, can be expressed conveniently in terms of the **f**-vector components, depending on the spin-dependent triplet pairing correlations as

$$f_x = \frac{1}{2} \left(-f_{\uparrow\uparrow} + f_{\downarrow\downarrow} \right)$$

$$f_y = -\frac{i}{2} \left(f_{\uparrow\uparrow} + f_{\downarrow\downarrow} \right) . \tag{13}$$

$$f_z = \frac{1}{2} \left(f_{\uparrow\downarrow} + f_{\downarrow\uparrow} \right)$$

The coordinate axis independent quantity, $|\mathbf{f}|^2$, can be interpreted as the mean density of spin-triplet Cooper pairs, and the quantity $i\mathbf{f} \times \mathbf{f}^*$ can be interpreted as a vector whose magnitude and direction denote the net spin moment arising from the non-unitary (equal-spin) part of the triplet Cooper pair density. Of course the quantities $|\mathbf{f}|$ and $i\mathbf{f} \times \mathbf{f}^*$ are also gauge invariant under overall phase changes of the superconducting order parameter.

3. Results and Discussion

3.1. Fixed α , fixed β

The results presented in this section are for pairing correlations at a SC/CM interface, obtained via a parameter scan of opening angle α and turning (or pitch) angle β in the ranges from 0° to 180°, calculated in steps of 5°. According to the definition (3) of α , conical magnetic structures with $\alpha < 90^{\circ}$ ($\alpha > 90^{\circ}$) have magnetic moment orientations pointing away (towards) the superconducting side of the interface. $\alpha = 90^{\circ}$ denotes the special case of a helical magnet with β , now known as the pitch angle. For the limiting cases with $\beta = 0^{\circ}$ ($\beta = 180^{\circ}$) the magnetic moments between adjacent layers are ordered ferromagnetically (antiferromagnetically), respectively.

The fundamental pairing amplitudes which we calculate are shown in figure 2, which shows results for a SC/CM interface containing Ho as the conical magnet, i.e. fixing $\alpha = 80^{\circ}$ and $\beta = 30^{\circ}$. The upper (lower) left panels show the real (green) and imaginary (orange) parts of the equal-spin (unequal-spin) spin-triplet correlations f_0 (f_1) as defined according to (7). The interface is indicated by the dashed line at

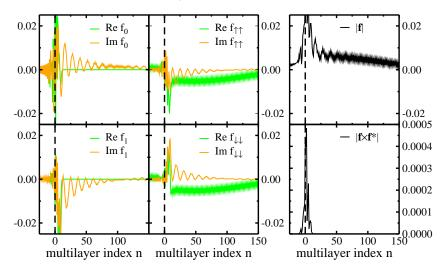


Figure 2. Real (green) and imaginary (orange) parts of the triplet pairing correlations f_0 (upper left panel) and f_1 (lower left panel) according to (7) for $\alpha=80\,^{\circ}$ and $\beta=30\,^{\circ}$. For better analysis the upper (lower) middle panels depict the real (green) and imaginary (orange) parts of $f_{\uparrow\uparrow}$ ($f_{\downarrow\downarrow}$) as components of f_1 shown in the lower left panel. Upper and lower right panels show the magnitude of the ${\bf f}$ -vector and the magnitude of ${\bf f}\times{\bf f}^*$ as introduced in (12), respectively. All data is shown depending on the multilayer index n, with the interface positioned at zero (dashed line).

layer n=0, with the superconductor on the left (layer n<0) and the CM on the right ($n\geq 0$). The upper (lower) middle panels depict the real (green) and imaginary (orange) parts of $f_{\uparrow\uparrow}$ ($f_{\downarrow\downarrow}$) for the same system. According to (7), these pairing correlations are the two contributions to f_1 . Finally, the upper and lower right panels of figure 2 depict the magnitude of the **f**-vector and the magnitude of $\mathbf{f} \times \mathbf{f}^*$ as introduced in (12), respectively.

Starting with f_0 and f_1 , shown in the left panels of figure 2, one notices only slight oscillations of the real parts around the interface layer, whereas the oscillations of the imaginary parts proceed well into the conical magnet layer. It has to be noted that the faster oscillations visible in the imaginary part are related to the chosen turning angle β , i.e., the layer index difference between adjacent maxima correspond to one full turn of the conical magnetic structure. This is superimposed on a slower oscillation responsible for some pronounced intensity decay in the imaginary parts of f_0 and f_1 as one goes further into the conical magnet side of the interface.

Looking now at the middle panels of figure 2, depicting the real and imaginary parts of $f_{\uparrow\uparrow}$ and $f_{\downarrow\downarrow}$, one notices a different behaviour for real and imaginary parts. The real parts of these quantities differ only in the interface region, and are of equal sign and size in parts of the conical magnet away form the interface. Evaluating f_1 according to (7) leads to the vanishing contributions away from the interface. The very fast oscillations shown in the real parts away from the interface are an artefact of the simple model used here and should vanish once the full \mathbf{k} dependence (parallel to the interface layer) and / or impurity scattering effects are taken into account, thereby allowing for deviations from the clean limit. The imaginary parts of $f_{\uparrow\uparrow}$ and $f_{\downarrow\downarrow}$, however, are of equal size but opposite sign leading to the nonvanishing contributions

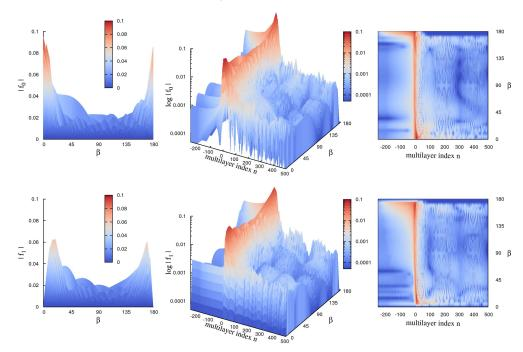


Figure 3. Influence of the turning angle β on the spin-triplet pairing correlations f_0 (upper panels) and f_1 (lower panels) as defined in (7) for fixed opening angle $\alpha=80\,^\circ$. Upper (lower) middle panels (logarithmic scale) depict full data sets of the magnitudes of f_0 (f_1), whereas in the left (linear scale) and right panels (logarithmic scale) the same data is shown when viewed from yz plane and as top view, respectively.

to f_1 shown in the lower left panel of figure 2.

The upper right panel of figure 2 depicts the corresponding magnitude of the \mathbf{f} -vector, as introduced in (12). The slightly out-of-phase relation between f_0 and f_1 leads to a faster oscillation in $|\mathbf{f}|$ compared to the oscillations in f_0 and f_1 alone. The very fast oscillations right of the interface stem from the contributions $f_{\uparrow\uparrow}$ and $f_{\downarrow\downarrow}$ as shown in the middle panels.

Finally the lower right panel in figure 2 depicts the magnitude of $\mathbf{f} \times \mathbf{f}^*$, giving insight in the spin magnetic properties of the Cooper pairs. It can be seen that the magnetic properties of the pairing decay very rapidly on both sides of the interface, with stronger intensities to be seen in the conical magnet side. The pairing spin magnetic moments are only visible for approximately one turn of the conical magnet, while the magnetic moments in the superconductor side of the interface describe the so-called inverse proximity effect.

3.2. Fixed α , general β

The influence of the turning angle β on the spin-triplet pairing correlations f_0 and f_1 is shown in the upper and lower panels of figure 3, respectively. Keeping the opening angle α fixed to 80° and allowing the turning angle β to vary between 0° and 180° yields the full data set depicted in the middle panels of figure 3 (logarithmic scale). The left (linear scale) and right panels (logarithmic scale) of figure 3 show the yz and

top view of the data shown in the middle panels, respectively.

In figure 3 the maximum values for any β clearly stem from the interface region, with a rapidly decaying oscillation in the conical magnet region. The influence of β on the pairing correlation f_0 is largest for $\beta=0^{\circ}$ and $\beta=180^{\circ}$, which is best seen from the upper left panel of figure 3. Going away from those extremal β values, the pairing correlation decays very quickly to approximately one third of its maximum value for $\beta=90^{\circ}$.

Looking at the f_1 pairing correlations in the lower panels of figure 3 the maxima are slightly shifted away from the extremal β values but show again a decrease towards $\beta = 90^{\circ}$ and fall again down to roughly one third of the maximum f_1 . In contrast to f_0 in the upper panels with maximal contributions from $\beta = 0^{\circ}$ and $\beta = 180^{\circ}$, the respective β contributions to f_1 vanish. The right panels show a top view of the data shown in the middle panels to depict the slight oscillations with changing β . These patterns are similar for f_0 and f_1 .

Keeping in mind that the data displayed in figure 3 corresponds to $\alpha=80^{\circ}$, the middle and right panels allow an estimate of the turning angle's influence on the decay length of f_0 and f_1 . Starting from the nonvanishing contributions to f_0 for $\beta=0^{\circ}$ ($\beta=180^{\circ}$) in the interface region, the decay length is largest (smallest) for the data shown here. For the other values of β the decay length has the same order of magnitude, being influenced by some oscillations due to the multilayer index n. Looking now at the f_1 values close to $\beta=0^{\circ}$ ($\beta=180^{\circ}$) in the interface region the decay length shows a similar behaviour to f_0 , being largest (smallest) for $\beta=0^{\circ}$ ($\beta=180^{\circ}$) values. Again, for the other values of β we observe decay lengths of the same order of magnitude and similar to the ones seen for f_0 .

Figure 4 now shows the influence of β on the magnitudes of the **f**-vector and $\mathbf{f} \times \mathbf{f}^*$, as introduced in (12), respectively. The upper panels present the magnitude of \mathbf{f} and the lower panels the magnitude of $\mathbf{f} \times \mathbf{f}^*$, each shown in the same parameter ranges and views as figure 3. Not surprisingly, the magnitude of the **f**-vector resembles the appearance of f_0 and f_1 from figure 3. The maxima occur for $\beta = 0^{\circ}$ and $\beta = 180^{\circ}$, as for f_0 , whereas the decaying patterns are similar to the ones already familiar from figure 3. Additionally, the most prominent contributions to the triplet pairing correlations again originate from the interface region. Only in the top view figure (upper right panel) can be seen a somewhat blurred superposition of the right panels of figure 3. This can be attributed to the slight out-of-phase relation of f_0 and f_1 , as already seen in figure 2 and discussed in section 3.1.

However, the magnitude of $\mathbf{f} \times \mathbf{f}^*$ describing the triplet spin magnetic properties behaves surprisingly differently. As seen in the lower panels of figure 4, it is zero for $\beta=0$ °, then increases up to a first maximum around $\beta=45$ °, and subsequently decreases again to form a small plateau around $\beta=90$ °. After that the magnitude of $\mathbf{f} \times \mathbf{f}^*$ has another sharp increase to its maximum value, before vanishing again for $\beta=180$ °. The fact that this vanishes for $\beta=0$ ° and $\beta=180$ ° is to be expected since these are collinear magnetic structures (ferro- or antiferromagnetic, respectively) and so there are no spin-flip processes at the SC/CM interface.

3.3. General α , general β

We now consider variations in the full range of both conical magnet angles α and varying β . As has been discussed in section 3.2 the most prominent contributions to either f_0 and f_1 or $|\mathbf{f}|$ and $|\mathbf{f} \times \mathbf{f}^*|$ originate from the interface region, as can be seen

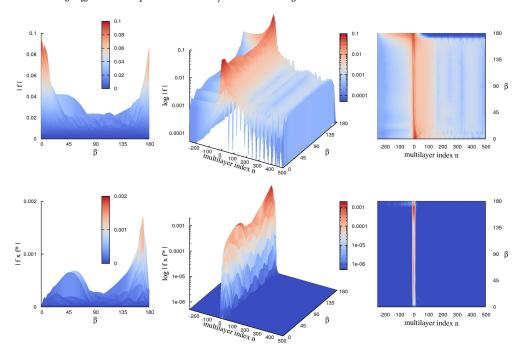


Figure 4. Influence of the turning angle β on the magnitude of the **f**-vector and $\mathbf{f} \times \mathbf{f}^*$ as defined in (12) for fixed opening angle $\alpha = 80^{\circ}$. Logarithmically scaled upper (lower) middle panels depict full data sets of the magnitudes of the **f**-vector $(\mathbf{f} \times \mathbf{f}^*)$, whereas in the left (linear scale) and right panels (logarithmic scale) the same data is shown when viewed from yz plane and as top view, respectively.

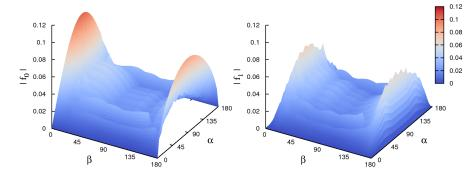


Figure 5. Left (right) panel: yz views of the magnitudes of f_0 (f_1) as depicted in the upper (lower) left panel of figure 4 for varying opening angle α .

clearly from figure 3 and figure 4. The height profile of the respective quantities for a fixed α and varying β are shown in the left panels of those figures, displaying the yz views. Since the maxima of f_0 and f_1 are always occurring in the interface region this gives us the opportunity to have a look at the data for all angles α and β . This is displayed in the plots shown in figure 5 with the left and right panels depicting the yz views of f_0 and f_1 now shown with varying opening angle α . As can be seen, for $\alpha = 0$ ° and $\alpha = 180$ ° the contributions to f_0 and f_1 vanish. With increasing α the triplet pairing correlations f_0 and f_1 increase up to a maximum around $\alpha = 90$ ° to

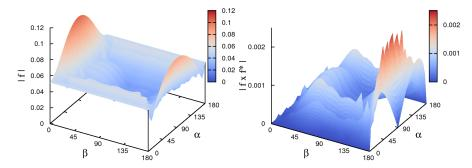


Figure 6. Left (right) panel: yz views of the magnitudes of the **f**-vector and $\mathbf{f} \times \mathbf{f}^*$ as depicted in the upper (lower) left panel of figure 5 for varying opening angle α .

then decay to zero again afterwards. In figure 5 the appearance along the β coordinate is similar for all α values and has already been shown, as for example in figure 3.

The full angle dependence on the magnitudes of the **f**-vector and $\mathbf{f} \times \mathbf{f}^*$ is shown in the left and right panels of figure 6, respectively. Focusing for the moment on the left panel showing the yz views of the magnitude of the **f**-vector one notices that for $\alpha = 0$ ° and $\alpha = 180$ ° it has a nonvanishing contribution, in contrast to the vanishing contributions of f_0 and f_1 depicted in figure 5. This can be understood knowing that vanishing contributions to f_1 are due to equal size but opposite sign contributions from $f_{\uparrow\uparrow}$ and $f_{\downarrow\downarrow}$ generating f_1 . Looking additionally at the separate contributions $f_{\uparrow\uparrow}$ and $f_{\downarrow\downarrow}$ can provide a deeper understanding of spin-triplet generation at specific interfaces. Coming back to the data at hand, maxima in the magnitude of the **f**-vector appear for $\alpha = 90$ ° and β either 0° or 180°, i.e., a complete ferromagnet or antiferromagnet with the magnetic moments oriented along the z-axis. All deviations from this ferromagnetic-like arrangement of magnetic moments between adjacent layers, either changing just β (corresponding to a helical magnet), or changing both α and β (a CM) leads to a decrease in the magnitude of the **f**-vector associated with the unitary triplet pairing correlations in the SC/CM interface.

The right panel of figure 6 now shows the magnitude of $\mathbf{f} \times \mathbf{f}^*$ associated with the non-unitary triplet pairing, or spin magnetic moment of the Cooper pair. The pattern of this quantity with respect to varying β are the same as already discussed in section 3.2 and shown in figure 4, namely vanishing contributions for $\beta = 0^{\circ}$, increase up to $\beta = 45^{\circ}$, again decreasing to the plateau around $\beta = 90^{\circ}$, and then the sharp increase to the maximum value. The maximum values of the non-unitary pairing correlations clearly occur for values of α near to 90° and $\beta = 180^{\circ}$, although the correlation becomes zero exactly at the point $\alpha = 90^{\circ}$, $\beta = 180^{\circ}$, since this is a antiferromagnetic structure.

One can see in these plots that the CM angle values of $\alpha=80\,^{\circ}$ and $\beta=30\,^{\circ}$, corresponding to Ho as used in the experiments, are fairly typical in their behaviour. In fact in figure 6 there is a broad maximum in the non-unitary triplet pairing function $\mathbf{f}\times\mathbf{f}^*$ for values similar to those of Ho.

4. Summary and Outlook

In summary, we have presented results on the spin-triplet pairing correlations in heterostructures built up from an s-wave superconductor and a general conical magnet described by an opening angle α and a turning (or pitch) angle β . All the results shown are obtained by self-consistent solutions of the microscopic Bogoliubov-de Gennes equations in the clean limit. The influence of the opening angle α and the turning (or pitch) angle β on the induced spin-triplet pairing correlations has been investigated in detail. We see that both unitary and non-unitary triplet pairing components are generated by any non-collinear magnetic structure, and that the CM values for Ho are typical of the behaviour over a very wide range of variations in these angles.

Acknowledgments

This work has been financially supported by the EPSRC (EP/I037598/1) and made use of computational resources of the University of Bristol. The authors gratefully acknowledge discussions with M. G. Blamire and J. W. A. Robinson on Ho containing heterostructures.

B. Györffy was an inspiration in the original plan for this project, and he was a co-investigator on this EPSRC grant. Sadly he passed away before the first results of this project were obtained.

References

- A. I. Buzdin. Proximity effects in superconductor-ferromagnet heterostructures. Rev. Mod. Phys., 77:935, 2005.
- [2] F. S. Bergeret, A. F. Volkov, and K. B. Efetov. Odd triplet superconductivity and related phenomena in superconductor-ferromagnet structures. Rev. Mod. Phys., 77:1321, 2005.
- [3] Y. Tanaka, M. Sato, and N. Nagaosa. Symmetry and Topology in Superconductors -Odd-Frequency Pairing and Edge States -. J. Phys. Soc. Japan, 81:011013, 2012.
- [4] M. Eschrig, T. Löfwander, T. Champel, J. C. Cuevas, J. Kopu, and G. Schön. Symmetries of Pairing Correlations in Superconductor-Ferromagnet Nanostructures. J. Low Temp. Physics, 147:457, 2007.
- [5] F. S. Bergeret, A. F. Volkov, and K. B. Efetov. Long-Range Proximity Effects in Superconductor-Ferromagnet Structures. *Phys. Rev. Lett.*, 86:4096, 2001.
- [6] I. Sosnin, H. Cho, V. T. Petrashov, and A. F. Volkov. Superconducting Phase Coherent Electron Transport in Proximity Conical Ferromagnets. Phys. Rev. Lett., 96:157002, 2006.
- [7] G. B. Halász, J. W. A. Robinson, J. F. Annett, and M. G. Blamire. Critical current of a Josephson juntion containing a conical magnet. Phys. Rev. B, 79:224505, 2009.
- [8] G. B. Halász, M. G. Blamire, and J. W. A. Robinson. Magnetic-coupling-dependent spin-triplet supercurrents in helimagnet/ferromagnet Josephson junctions. *Phys. Rev. B*, 84:024517, 2011.
- [9] J. W. A. Robinson, J. D. S. Witt, and M. G. Blamire. Controlled Injection of Spin-Triplet Supercurrents into a Strong Ferromagnet. Science, 329:59, 2010.
- [10] M. Alidoust, J. Linder, G. Rashedi, T. Yokoyama, and A. Sudbø. Spin-polarized Josephson current in superconductor/ferromagnet/superconductor junctions with inhomogeneous magnetization. *Phys. Rev. B*, 81:014512, 2010.
- [11] C.-T. Wu, O. T. Valls, and K. Halterman. Proximity effects in conical-ferromagnet/superconductor bilayers. *Phys. Rev. B*, 86:184517, 2012.
- [12] D. Fritsch and J. F. Annett. Proximity effect in superconductor/conical magnet/ferromagnet heterostructures. New J. Phys., 16:055005, 2014.
- [13] O. Šipr and B. L. Györffy. Oscillatory magnetic coupling between metallic multilayers across superconducting spacers. *J. Phys.: Condens. Matter*, 7:5239, 1995.
- [14] J. F. Annett. Superconductivity, Superfluids and Condensates. Oxford University Press, Oxford, 2004.

- [15] J. B. Ketterson and S. N. Song. Superconductivity. Cambridge University Press, Cambridge, 1999.
- [16] L. Covaci and F. Marsiglio. Proximity effect and Josephson current in clean strong/weak/strong superconducting trilayers. Phys. Rev. B, 73:014503, 2006.
- [17] R. Balian and N. R. Werthamer. Superconductivity with pairs in a relative p wave. Phys. Rev., 131:1553, 1963.
- [18] M. Sigrist and K. Ueda. Phenomenological theory of unconventional superconductivity. Rev. Mod. Phys., 63:239, 1991.
- [19] K. Halterman, P. H. Barsic, and O. T. Valls. Odd Triplet Pairing in Clean Superconductor/Ferromagnet Heterostructures. Phys. Rev. Lett., 99:127002, 2007.
- [20] S. Kawabata, Y. Asano, Y. Tanaka, and A. A. Golubov. Robustness of Spin-Triplet Pairing and Singlet-Triplet Pairing Crossover in Superconductor/Ferromagnet Hybrids. J. Phys. Soc. Japan, 82:124702, 2013.